Daytime forecast of optical turbulence for optical communications

Florian Quatresooz, Danielle Vanhoenacker-Janvier, and Claude Oestges

ICTEAM Institute, Université catholique de Louvain (UCLouvain), Louvain-la-Neuve, Belgium

ABSTRACT

In recent years, forecast of optical turbulence has been developed for astronomical sites. It enables flexible scheduling of observations during the night, and improves the control of adaptive optics systems. Nowadays, there is also a need for optical turbulence forecast during daytime at locations considered for future satellite-to-ground optical communications, for example in cities. In this work, a numerical approach to forecast refractive index structure parameter (C_n^2) profiles for optical communication sites is presented. It relies on the Weather Research and Forecasting software, with the boundary layer considered separately. Indeed, it is shown that during daytime and at non-astronomical sites, the boundary layer has a great impact on seeing conditions. This motivates the use of hybrid C_n^2 profiles, separating the free atmosphere from the surface layer. This approach is applied to Tenerife, Spain, where the European Space Agency has already built an optical ground station. Measurements of integrated parameters (seeing) are available at this location, and are compared with the forecast integrated parameters. The current limitations of the model can thereby be highlighted.

Keywords: Free space optics, optical turbulence, Numerical Weather Prediction

1. INTRODUCTION

The effects of atmospheric turbulence on the propagation of optical waves, referred to as optical turbulence, have been studied at astronomical sites for several decades.[1] Various models of the refractive index structure parameter C_n^2 have been presented (e.g. Hufnagel-Valley model,[2] Tatarskii models,[3] Trinquet-Vernin model,[4] etc.), and tools enabling to forecast C_n^2 profiles have also been developed, thanks to numerical weather prediction (NWP) software.[5,6]

Furthermore, optical turbulence is also a concern for the development of future ground-to-satellite optical communications. Its forecast at the locations of future optical ground stations (OGS) is expected to be more challenging, for two reasons: OGS may not be located at the ideal locations of observatories,[7] and optical communications will also take place during daytime, and not only during nighttime.

This paper focuses on the second challenge, i.e., the forecast of optical turbulence during daytime. This effect has rarely been studied at astronomical sites, except for solar observatories.[8,9] Daytime turbulence is increased in the boundary layer, namely due to convection from solar heating of the ground.[2] In order to accurately describe this boundary layer, models based on the turbulent kinetic energy (TKE) have been explored.[7] Alternatively, hybrid C_n^2 profile models have been suggested in the literature, that consider the boundary layer and the free atmosphere differently.[10,11] The boundary layer C_n^2 models involve the ground C_n^2 value, often obtained empirically,[12,13] or thanks to Monin-Obukhov similarity theory.[14,15]

The OGS location considered in this work is actually an astronomical site, being the Teide Observatory at Tenerife, Spain, where an ESA optical ground station has been deployed. Seeing measurements have been collected during daytime at this location, and are used to validate optical turbulence prediction models. Section 2 presents the NWP software parameterisation, as well as the chosen C_n^2 models. Then, Section 3 compares seeing forecasts from the C_n^2 models with the measurements.

2. FORECAST OF OPTICAL TURBULENCE QUANTITIES

Relying on NWP simulations, one can forecast meteorological quantities in the future, above a location of interest. Similarly, such simulations can be used to enhance the spatial and temporal resolutions of past recorded meteorological data.[7] In this work, the second approach is chosen: ERA5 reanalysis data from ECMWF[16] are used to initialize Weather Research and Forecasting[17] (WRF) simulations above Tenerife, for the month of July 2021. Then, from the forecast meteorological quantities, C_n^2 profiles are obtained.

2.1 NWP simulations

The conducted NWP simulations are centered on the ESA optical ground station at Teide Observatory, Tenerife, Spain (latitude 28°18′03″N, longitude 16°30′43″W, altitude 2400 m). Three nested domains, detailed in Table 1, enable to reach a horizontal resolution of 1 km, while 80 levels are used vertically. Those levels are distributed between the ground and the top pressure of the atmosphere, set to 5000 Pa, with smaller level spacing close to the ground. For each day, simulations are started at 18h00 the day before, ensuring a lead time of 6 hours. Then, outputs are saved every 5 minutes above the location of interest, for the full day (i.e., from 00h00 to 00h00 the next day).

Table 1: Grid parameters from WRF simulations.

Domain	Grid resolution (km)	Number of grid points	Domain size (km)	Number of vertical levels
d01	9	112×112	1008×1008	80
d02	3	112×112	336×336	80
d03	1	112×112	112×112	80

WRF configuration makes use of the following physical schemes: WSM6[18] for microphysics, Tiedtke[19] for cumulus physics (only in domain d01), Dudhia[20] and RRTM[21] for shortwave and longwave radiations, revised MM5[22] for the surface layer, and MYNN 2.5[23] for planetary boundary layer physics.

2.2 C_n^2 models

Two different parametric models of C_n^2 are considered. The first one relies on the TKE, that is directly retrieved in WRF outputs. The second model makes use of the Tatarskii expression, completed by a boundary layer model.

TKE model The chosen TKE model comes from Ref. 5, and has been extensively used for astronomical applications, namely with Astro-Meso-Nh.[5,24] Its implementation with WRF is detailed in Ref. 7. Thanks to the dependency of the model with the TKE, it is expected to provide a description of optical turbulence in the boundary layer, close to the ground.

Tatarskii-based model This second model relies on Tatarskii equation,[3]

$$C_{n,\mathrm{Tat}}^2(z) = a^2 L_0^{4/3} M^2, \tag{1}$$

with $a^2 = 2.8$,[25] and $M = \frac{\partial n}{\partial z}$ equal to[26]

$$M = -\frac{80 \times 10^{-6} p}{T\theta} \frac{\partial \theta}{\partial z}. \tag{2}$$

In this expression, T is the temperature [K], p is the pressure [hPa], θ is the potential temperature [K], n is the refractive index, and z is the altitude [m]. Regarding the outer scale L_0, the HMNSP99 model is used[27,28]

$$L_0^{4/3} = 0.1^{4/3} \times 10^{Y} \text{ with } Y = \begin{cases} 0.362 + 16.728\, S - 192.347\, \frac{\partial T}{\partial z} \text{ in the troposphere,} \\ 0.757 + 13.819\, S - 57.784\, \frac{\partial T}{\partial z} \text{ in the stratosphere.} \end{cases} \tag{3}$$

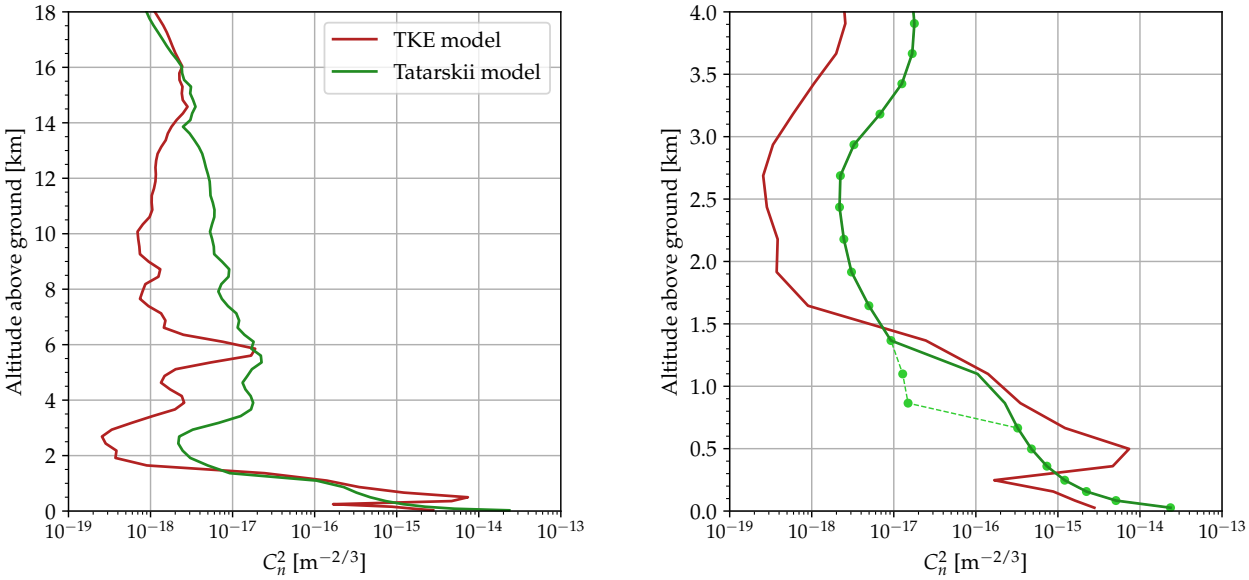

Figure 1: Modelled C_n^2 profiles at Tenerife for July 15, 2021, at 12h00 UTC.

This model is empirical, based on measurements in New Mexico, USA. S is the vertical shear of the horizontal wind velocity, and the tropopause height, i.e., the limit between the troposphere and the stratosphere, is set at 14 km of altitude above ground. The quantities involved in Eqs. (2) and (3) are functions of the altitude z, such that a vertical $C_n^2(z)$ profile is obtained.

The Tatarskii-based model from Eq. (1) has been found to underestimate C_n^2 in the boundary layer. Hence, it is complemented by a boundary layer C_n^2 model, derived from the Monin-Obukhov similarity theory.[14,29] The implementation of this model in WRF has been presented in Ref. 30. It offers an estimation of C_n^2 in the ground layer from the sensible heat flux, the latent heat flux, the friction velocity $u^\star$, and the 2-meter temperature. All those parameters are available in WRF simulation outputs such that, from the equations in Refs. 14 and 30, C_n^2 at two meters above ground ($z = 2$ m) is computed, denoted $C_{n,\mathrm{gr}}^2$.

From this ground C_n^2 value, a $C_n^2(z)$ profile is computed up to the height of the planetary boundary layer h_{BL} using a decrease rate of $z^{-4/3}$. This corresponds to the daytime trend of C_n^2 profiles in the atmospheric boundary layer dominated by convection.[2] The height of the boundary layer is a WRF state variable, provided in WRF output files.

Finally, continuity between the boundary layer C_n^2 profile and the Tatarskii-based model in the free atmosphere is ensured thanks to a linear interpolation, from h_{BL} up to $h_{\mathrm{BL}} + \Delta h$. As a result, the $C_n^2(z)$ profile is given by

$$C_n^2(z) = \begin{cases} C_{n,\mathrm{gr}}^2 \cdot \left(\frac{z}{2}\right)^{-4/3} & \text{for } z \leq h_{\mathrm{BL}}, \\ C_{n,\mathrm{gr}}^2 \cdot \left(\frac{h_{\mathrm{BL}}}{2}\right)^{-4/3} \frac{h_{\mathrm{BL}}+\Delta h-z}{\Delta h} + C_{n,\mathrm{Tat}}(z) \frac{z-h_{\mathrm{BL}}}{\Delta h} & \text{for } h_{\mathrm{BL}} < z \leq h_{\mathrm{BL}} + \Delta h, \\ C_{n,\mathrm{Tat}}(z) & \text{for } z > h_{\mathrm{BL}} + \Delta h. \end{cases} \tag{4}$$

The TKE and Tatarskii-based C_n^2 models are illustrated in Figure 1 for July 15, 2021, at 12h00 UTC. The right part of the figure focuses on the boundary layer (with $h_{\mathrm{BL}} = 850$ m at this particular time), and highlights (with the dots and dash line) the interpolation between the Tatarskii profile (top) and the boundary layer profile (bottom). A distance $\Delta h = 0.5\, h_{\mathrm{BL}}$ has been chosen.

3. COMPARISON WITH SEEING MEASUREMENTS AT TENERIFE

Measurements of seeing have been collected by a Miratlas' Sky Monitor* installed at Teide Observatory, next to the ESA optical ground station. From the simulated meteorological quantities given by WRF, C_n^2 profiles are computed every 5 minutes, and integrated to obtain the seeing ϵ_0, according to

$$\epsilon_0 = 5.285\lambda^{-1/5} \left(\sec(\xi) \int_{h_0}^{\infty} C_n^2(z)\, \mathrm{d}z \right)^{3/5}, \tag{5}$$

where h_0 is the altitude of the first WRF level, $\xi = 0°$ is the elevation angle measured from zenith, and $\lambda = 500$ nm is the wavelength.

Measured and predicted seeing for the month of July 2021 are given in Figure 2. Seeing measurements are collected every minute, before being grouped in bins of 5 minutes. The mean of each bin is depicted in blue, while the area shaded in blue corresponds to the mean plus (minus) the standard deviation. Data is only available during the day, and nights correspond to the areas in gray. The label of the day is set at 00h00 UTC for the day. Some days with seeing measurements larger than 3 arcsec have been discarded, as they have been associated to cloudy days.

In Figure 2, one can notice that the magnitudes of the estimated seeing from the TKE and the Tatarskii-based models are in agreement with the measurements for most of the days (except for some predictions from the TKE model during the last ten days of July 2021). Moreover, the daytime variation, i.e., the increase of the seeing from sunrise to approximately noon and then its decrease up to the sunset, is also modelled. The correlation plots between the measurements and the predicted values (from Figure 2, hence every 5 minutes) are given in Figure 3. In these plots, the overestimation of the seeing from the TKE model for some days is noticeable. A correlation coefficient of 0.56 is obtained for the TKE model, while a value of 0.53 is reached for the Tatarskii-based model. A root-mean-square error (RMSE) of 0.80 arcsec (resp. 0.43 arcsec) is computed with the TKE model (resp. Tatarskii-based model).

Finally, distributions of measured/modelled seeing are presented in Figure 4, along with the cumulative density function (CDF) in Figure 4d. The mean of the distribution μ is given in the legend, as well as the standard deviation σ. The mean is also depicted in black on the histograms, while the median is in cyan. Measurements tend to be symmetric around the mean of their distribution, while the predictions are skewed towards lower seeing values. Large seeing values are also obtained with the TKE model. As a result, the cumulative density distributions of the predicted seeing do not exactly follow the one of the measurements.

4. CONCLUSION

In order to forecast seeing during daytime, an accurate description of the C_n^2 profile in the boundary layer is required. In this work, it is achieved either using a C_n^2 model directly based on the turbulent kinetic energy, or from a Tatarskii-based model complemented with a boundary layer profile inspired from Monin-Obukhov similarity theory.

Those two models can depict daytime variations of optical turbulence, and compare well with seeing measurements at Tenerife. However, their correlations with measurements can still be improved, and the predicted distributions do not perfectly match the distribution of the measurements.

Possible limitations of the presented approach are associated to the accuracy of the prediction of NWP simulations, and to the difficulty of modelling short-term phenomena. Hence, alternative approaches, such as autoregressive models,[31] can be considered for modelling of short-term seeing variations, by combining NWP results with real-time measurements.

*https://www.miratlas.com/

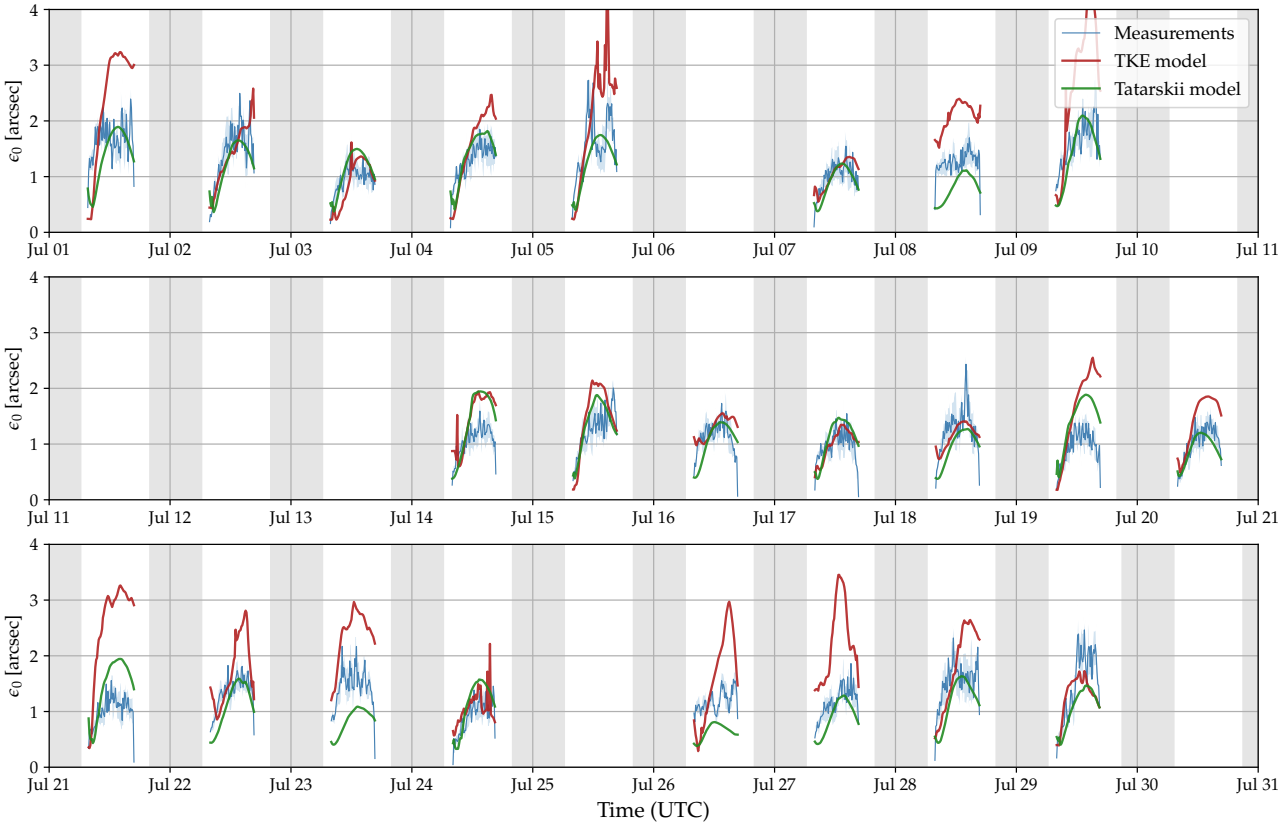

Figure 2: Seeing measurements and predictions for the month of July 2021, at Tenerife.

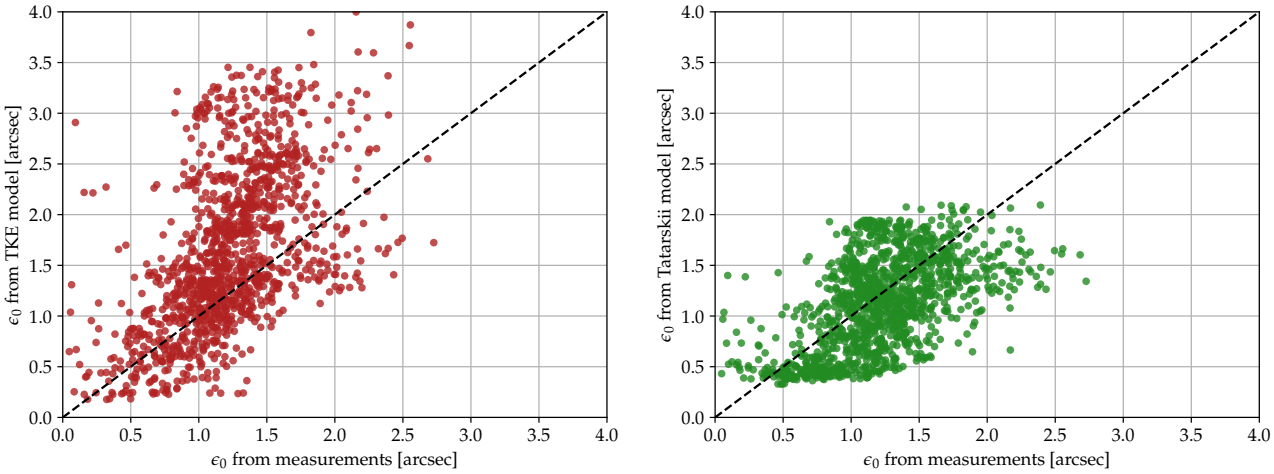

(a) TKE model

(b) Tatarskii model

Figure 3: Correlation plots between seeing measurements and their predictions.

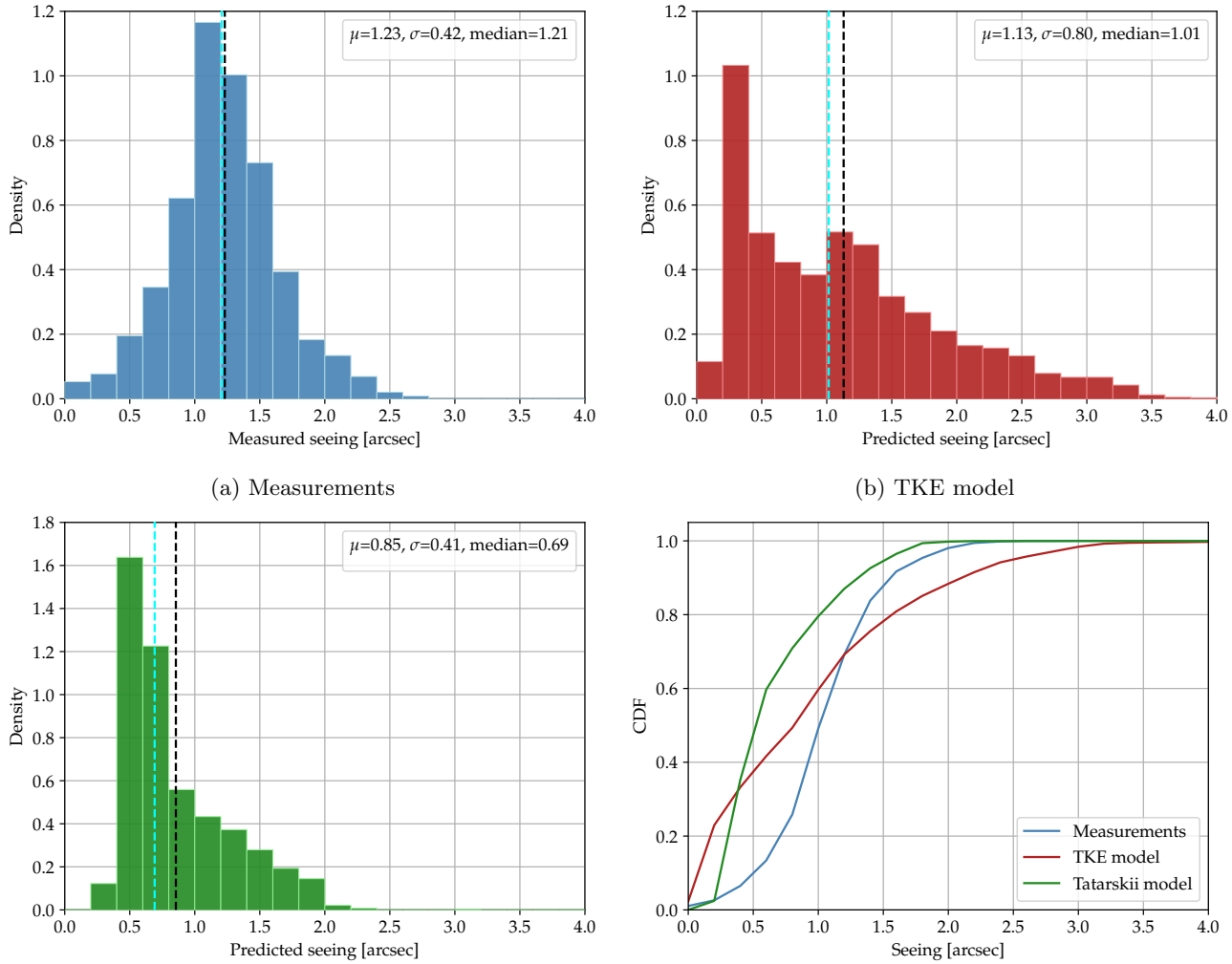

(a) Measurements

(b) TKE model

(c) Tatarskii model

(d) CDF

Figure 4: Distributions of measured and modelled seeing.

ACKNOWLEDGMENTS

The authors thank Jean-Edouard Communal and Frédéric Jabet from Miratlas for giving access to their seeing measurements at Tenerife. Szymon Gładysz, Detlev Sprung, and Carmen Ullwer, are also thanked for the fruitful discussions on the topic of this paper.

REFERENCES

[1] Roddier, F., "V The effects of atmospheric turbulence in optical astronomy," in [*Progress in optics*], **19**, 281–376, Elsevier (1981).

[2] Andrews, L. C. and Phillips, R. L., [*Laser Beam Propagation through Random Media, Second Edition*], SPIE Press (2005).

[3] Tatarskii, V. I., "The effects of the turbulent atmosphere on wave propagation," *Jerusalem: Israel Program for Scientific Translations, 1971* (1971).

[4] Trinquet, H. and Vernin, J., "A statistical model to forecast the profile of the index structure constant C_N^2," *Environmental Fluid Mechanics* **7**(5), 397–407 (2007).

[5] Masciadri, E., Vernin, J., and Bougeault, P., "3D mapping of optical turbulence using an atmospheric numerical model-I. a useful tool for the ground-based astronomy," *Astronomy and Astrophysics Supplement Series* **137**(1), 185–202 (1999).

[6] Osborn, J. and Sarazin, M., "Atmospheric turbulence forecasting with a general circulation model for Cerro Paranal," *Monthly Notices of the Royal Astronomical Society* **480**(1), 1278–1299 (2018).

[7] Quatresooz, F., Orban de Xivry, G., Absil, O., Vanhoenacker-Janvier, D., and Oestges, C., "Challenges for optical turbulence characterization and prediction at optical communication sites," International Conference on Space Optics (ICSO) 2022 (2022).

[8] Sprung, D. and Sucher, E., "Characterization of optical turbulence at the solar observatory at the mount teide, tenerife," in [*Remote Sensing of Clouds and the Atmosphere XVIII; and Optics in Atmospheric Propagation and Adaptive Systems XVI*], **8890**, 321–329, SPIE (2013).

[9] Montoya, L., De La Rosa, J., Castro-Almazán, J., Montilla, I., and Collados, M., "Modeling day time turbulence profiles: application to teide observatory," *Adaptive Optics for Extremely Large Telescopes (AO4ELT5)* (2017).

[10] Robert, C., Velluet, M.-T., Masciadri, E., Turchi, A., Conan, J.-M., Védrenne, N., Artaud, G., and Benammar, B., "Characterization of the turbulent atmospheric channel of space-ground optical links with parametric models: description and cross-validation with mesoscale models and in situ measurements," in [*Environmental Effects on Light Propagation and Adaptive Systems II*], **11153**, 15–26, SPIE (2019).

[11] Vedrenne, N., Petit, C., Montmerle-Bonnefois, A., Lim, C., Conan, J.-M., Paillier, L., Velluet, M.-T., Caillault, K., Gustave, F., Durecu, A., et al., "Performance analysis of an adaptive optics based optical feeder link ground station," in [*International Conference on Space Optics—ICSO 2020*], **11852**, 527–535, SPIE (2021).

[12] Sadot, D. and Kopeika, N. S., "Forecasting optical turbulence strength on the basis of macroscale meteorology and aerosols: models and validation," *Optical Engineering* **31**(2), 200–212 (1992).

[13] Bendersky, S., Kopeika, N. S., and Blaunstein, N., "Atmospheric optical turbulence over land in middle east coastal environments: prediction modeling and measurements," *Applied optics* **43**(20), 4070–4079 (2004).

[14] Andreas, E. L., "Estimating cn 2 over snow and sea ice from meteorological data," *JOSA A* **5**(4), 481–495 (1988).

[15] Tunick, A., "Cn2 model to calculate the micrometeorological influences on the refractive index structure parameter," *Environmental Modelling & Software* **18**(2), 165–171 (2003).

[16] Copernicus Climate Change Service (C3S), "ERA5: Fifth generation of ECMWF atmospheric reanalyses of the global climate," (2017). Copernicus Climate Change Service Climate Data Store (CDS), *Accessed 16 June 2021*, https://cds.climate.copernicus.eu/cdsapp#!/home.

[17] Skamarock, W. C., Klemp, J. B., Dudhia, J., Gill, D. O., Liu, Z., Berner, J., Huang, X. -yu., "A Description of the Advanced Research WRF Model Version 4," (2019). (No. NCAR/TN-556+STR). http://dx.doi.org/10.5065/1dfh-6p97.

[18] Hong, S.-Y. and Lim, J.-O. J., "The WRF single-moment 6-class microphysics scheme (WSM6)," *Asia-Pacific Journal of Atmospheric Sciences* **42**(2), 129–151 (2006).

[19] Zhang, C., Wang, Y., and Hamilton, K., "Improved representation of boundary layer clouds over the southeast Pacific in ARW-WRF using a modified Tiedtke cumulus parameterization scheme," *Monthly Weather Review* **139**(11), 3489–3513 (2011).

[20] Dudhia, J., "Numerical study of convection observed during the winter monsoon experiment using a mesoscale two-dimensional model," *Journal of Atmospheric Sciences* **46**(20), 3077–3107 (1989).

[21] Mlawer, E. J., Taubman, S. J., Brown, P. D., Iacono, M. J., and Clough, S. A., "Radiative transfer for inhomogeneous atmospheres: RRTM, a validated correlated-k model for the longwave," *Journal of Geophysical Research: Atmospheres* **102**(D14), 16663–16682 (1997).

[22] Jiménez, P. A., Dudhia, J., González-Rouco, J. F., Navarro, J., Montávez, J. P., and García-Bustamante, E., "A revised scheme for the WRF surface layer formulation," *Monthly Weather Review* **140**(3), 898–918 (2012).

[23] Nakanishi, M. and Niino, H., "Development of an improved turbulence closure model for the atmospheric boundary layer," *Journal of the Meteorological Society of Japan. Ser. II* **87**(5), 895–912 (2009).

[24] Masciadri, E., Lascaux, F., Turchi, A., and Fini, L., "Optical turbulence forecast: ready for an operational application," *Monthly Notices of the Royal Astronomical Society* **466**(1), 520–539 (2017).

[25] Beland, R. R. and Brown, J. H., "A deterministic temperature model for stratospheric optical turbulence," *Physica Scripta* **37**(3), 419 (1988).

[26] Cherubini, T., Businger, S., and Lyman, R., "Modeling optical turbulence and seeing over Mauna Kea: Verification and algorithm refinement," *Journal of Applied Meteorology and Climatology* **47**(12), 3033–3043 (2008).

[27] Dewan, E. M., [*A Model for C2n (optical turbulence) profiles using radiosonde data*], no. 1121, Directorate of Geophysics, Air Force Materiel Command (1993).

[28] Ruggiero, F. H. and DeBenedictis, D. A., "Forecasting optical turbulence from mesoscale numerical weather prediction models," in [*DoD High Performance Modernization Program Users Group Conference*], 10–14 (2002).

[29] Stull, R. B., [*An introduction to boundary layer meteorology*], vol. 13, Springer Science & Business Media (1988).

[30] Ullwer, C., Sprung, D., Sucher, E., Kociok, T., Grossmann, P., van Eijk, A. M., and Stein, K., "Global simulations of Cn2 using the Weather Research and Forecast Model WRF and comparison to experimental results," in [*Laser Communication and Propagation through the Atmosphere and Oceans VIII*], **11133**, 126–136, SPIE (2019).

[31] Masciadri, E., Martelloni, G., and Turchi, A., "Filtering techniques to enhance optical turbulence forecast performances at short time-scales," *Monthly Notices of the Royal Astronomical Society* **492**(1), 140–152 (2020).